Physical modeling of flows in black liquor recovery boilers

Stephen P. Ketler, Michael C. Savage, and Ian S. Gartshore

ABSTRACT: Flow patterns inside kraft recovery boilers are difficult to measure or visualize directly. As an aid to understanding the flow in actual boilers, detailed velocity measurements were made using a laser Doppler velocimeter in a small-scale physical model of a black liquor recovery boiler. Water at room temperature was used as the fluid in the model, which included representation of the boiler tube bank but not the smelt bed. For the load-burner (above liquor guns) upper furnace flow arrangement, the central vertical core flow traditionally expected was not observed. An asymmetrical flow pattern dominated, with upflow near the front and side walls and downflow or recirculation elsewhere. This general flow pattern was insensitive to minor configuration changes in the furnace. Results were essentially independent of total mass flow rate and contained large amplitude unsteadiness.

KEYWORDS: Black liquors, Doppler effect, flow, lasers, measuring instruments, models, recovery furnaces, simulation, velocity indicators, velocity measurement.

The understanding of flow inside black liquor recovery boilers has been limited due to its complex nature. The interaction of hundreds of jets in crossflow defies analytical solutions while pushing the capabilities of present-day computational fluid dynamics to their limits *(1)*. Thus physical modeling is an essential tool for understanding recovery boiler flows.

The main variables affecting boiler efficiency, and hence capacity, are the physical arrangement of the combustion air ports, the proportion of combustion air mass flow among the different port levels, and the arrangement for air injection into the furnace at each level. The first variable is not readily altered for a commissioned boiler, but the last two may be changed with relative ease by operators in the field. There is a great deal of experience in the efficient operation of specific boilers, but there is less ability to predict the effects of changes in air flow ratios or arrangements. The flow field affects the degree of mixing of the combustible organics with available oxygen, determining the overall rate of combustion. Information on the flow field in the boiler is therefore directly related to efficiency and capacity.

Measurement of flow patterns and velocities in full-scale operating boilers is extremely difficult due to the high temperature of the environment and problems with fouling of physical probes by char, fume, or entrained liquor droplets; certain operational functions such as sootblowing must also be accommodated. The advantages of using a model sufficiently representative of the real furnace for experimental investigations are therefore significant.

The objectives of this experimental study are twofold. First, results may be used for evaluating different flow configurations for full-scale boilers and may be compared to results from isothermal model tests by other investigators. Second, results may be used to validate the isothermal portion of a computational fluid dynamics code for boiler flow. This code is currently under development at the University of British Columbia (UBC).

The use of isothermal scale models of boilers to simulate full-scale operating conditions has met with success on numerous occasions *(2, 3)* and forms the basis of this investigation. The value of such physical air flow modeling has been demonstrated by other researchers *(4)*. Due to the high tur-

Ketler is a graduate student, Savage is a research engineer, and Gartshore is a professor in the Department of Mechanical Engineering at the University of British Columbia, Vancouver, BC, Canada V6T 1Z4.

bulence of the flow, a nonintrusive measurement technique capable of recording the instantaneous velocity direction and magnitude is particularly useful. Multi-hold pitot-static tubes *(5)* suffer from orientation difficulties, are disruptive to the flow, have low temporal resolution, and therefore have limited applications. Measurement devices such as the pulsed hot wire *(6)* are capable of distinguishing instantaneous velocity vectors, but they are disruptive to a highly turbulent flow of this nature and are rather fragile.

A method capable of accurately measuring unsteady velocities, while not physically altering the flow, is the laser Doppler velocimeter (LDV) *(7)*. The LDV is able to simultaneously measure multiple components of velocity at a single point, with both high temporal and spatial resolutions. This technique requires that light be scattered from small particles that accurately follow the flow. For this reason, the working fluid in the model was chosen to be water as opposed to air. The suitability for using methods of flow visualization to complement the LDV also favors water over air. Furthermore, the use of a water analog to simulate a gaseous internal flow has been shown to be a valid representation for many situations *(8, 9)*.

1. Recovery boiler water model facility

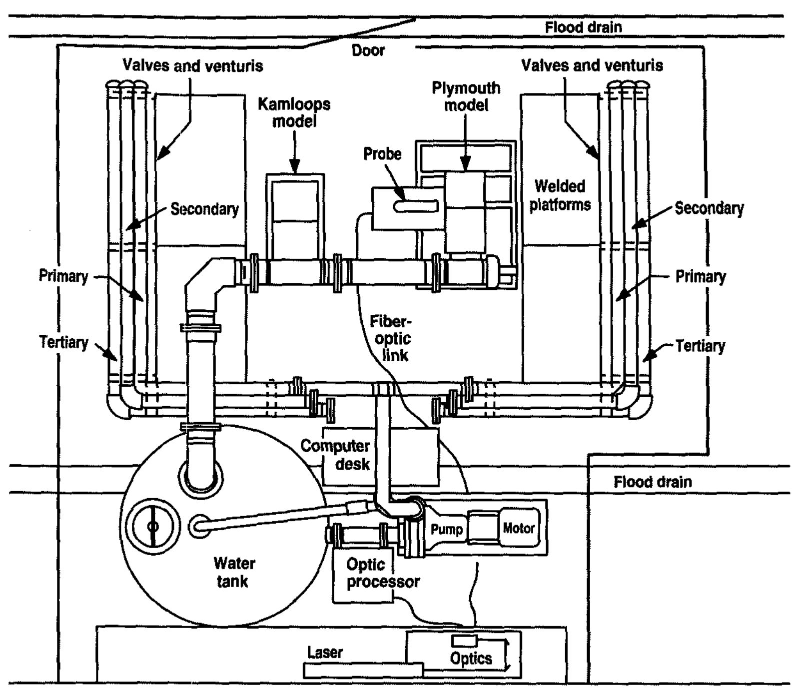

Experimental program

A physical flow facility, consisting of two 1/28-scale boiler models running water at room temperature, has been constructed at the UBC Pulp and Paper Centre. The first model represents a boiler located in Plymouth, NC, originally commissioned by Combustion Engineering. The second model is that of a facility in Kamloops, BC, originally designed by Babcock and Wilcox. Both boilers are owned and operated by the Weyerhaeuser Paper Co. Only work involving the first model will be considered here.

A plan view of the experimental facility is shown in **Fig. 1.** A 40-hp centrifugal pump draws water from a 4200-L reservoir, sending it vertically into three headers feeding the primary, secondary, and load-burner or tertiary model ports, respectively. Flow control is achieved by adjusting two gate valves; one controls a bypass line while the other throttles flow into the headers. A total of 59 lines of 0.625-in. flexible hose lead water from the header pipes through a valve and orifice plate flowmeter. The hoses then lead to manifolds feeding four to nine ports each, with the exception of the load-burner ports, which are connected directly to the headers. To set up a given flow condition, a differential pressure meter is attached to each flowmeter in turn,

I. No. of recovery boiler ports

Air port	*No. of ports*
Primary	156
Starting-burner	4
Secondary	66
Tertiary	28
Load-burner	10

2. Plymouth boiler port arrangement

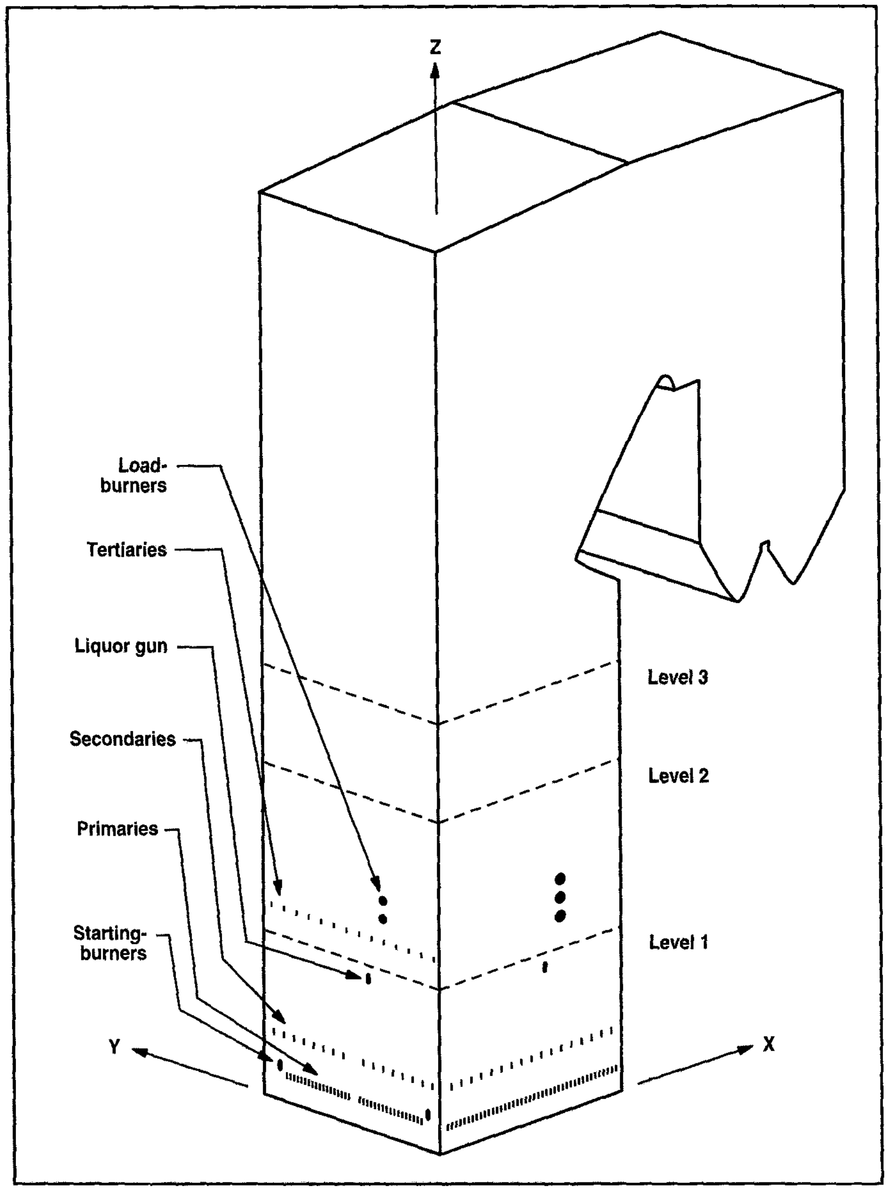

II. Model flow results

Run	Level	Pred. flow, L/min	Meas. flow, L/min	Meas. $\overline{w}$, m/s	Meas. $\overline{K}^{1/2}$ m/s		Configuration*
A	1	437	437	0.0482	0.1553	LB - 23%	1 port/wall
	2	568	537	0.0593	0.1130	S - 40%	
	3	568	534	0.0589	0.0953	P - 33%	SB - 4%
B	1	219	253	0.0279	0.0835	LB - 23%	2 ports/wall
	2	284	265	0.0292	0.0528	S - 40%	
	3	284	289	0.0319	0.0456	P - 37%	
C	1	437	451	0.0498	0.1545	LB - 23%	1 port/wall
	2	568	573	0.0633	0.1054	S - 40%	No boiler tubes
	3	568	550	0.0607	0.0856	P - 33%	SB - 4%

*LB=load-burner, S=secondary, P=primary, SB=starting-burner

and the corresponding valve is adjusted to achieve the desired flow rates.

The full-scale boiler is approximately 140 ft high by 36 ft square and features one liquor gun on each wall. The model is constructed of 0.188-in. plexiglass, and all ports present in the full-scale boiler are modeled. Liquor flow into and smelt flow out of the boiler are not modeled. It is assumed that the mass flux of each flow is approximately equal, and any influence of the liquor droplets or their combustion products on the flow patterns or velocities is neglected. The smelt bed itself is not presently included in the model. Four starting burners are located at the corners of the front and rear faces at the primary level, angled 25° toward the boiler center. Primary air ports are angled 10° down from horizontal, while the secondary air systems are of traditional configuration. The third level ports may be configured in one of two ways: load-burner (sometimes referred to as high-secondary) air ports are directed along the tangent of an imaginary horizontal circle located above the liquor gun level, while tertiary air ports on the front and rear faces may be used in either opposed or interlaced configurations. The number of ports is summarized in **Table I**, while the boiler configuration and measurement coordinate system are illustrated in **Fig. 2**.

In the actual furnace, the combustion air enters at a temperature of approximately 150°C, while the temperature in the furnace is about 1000°C. The density change that the combustion air in the full-scale furnace undergoes cannot be simulated in an isothermal water model. In some models, ports are enlarged to preserve momentum flux ratios between model and full-scale; the ports in the Plymouth model are 1/28 scale. If the mass flux ratio between vertical flow in the furnace and port flow is maintained between the full-scale and model, then the velocity ratio between model and full-scale is:

$$(V_p/V_v)_{fs} = (\rho_v/\rho_p)_{fs} \times (V_p/V_v)_{model} \quad (1)$$

3. Two components of mean and RMS velocities—Run A. (a): RMS *u* and *w* velocities are shown as crosses originating from the base of each mean velocity vector, (b) through (d): *u* velocity component alone is shown for the three measurement levels.

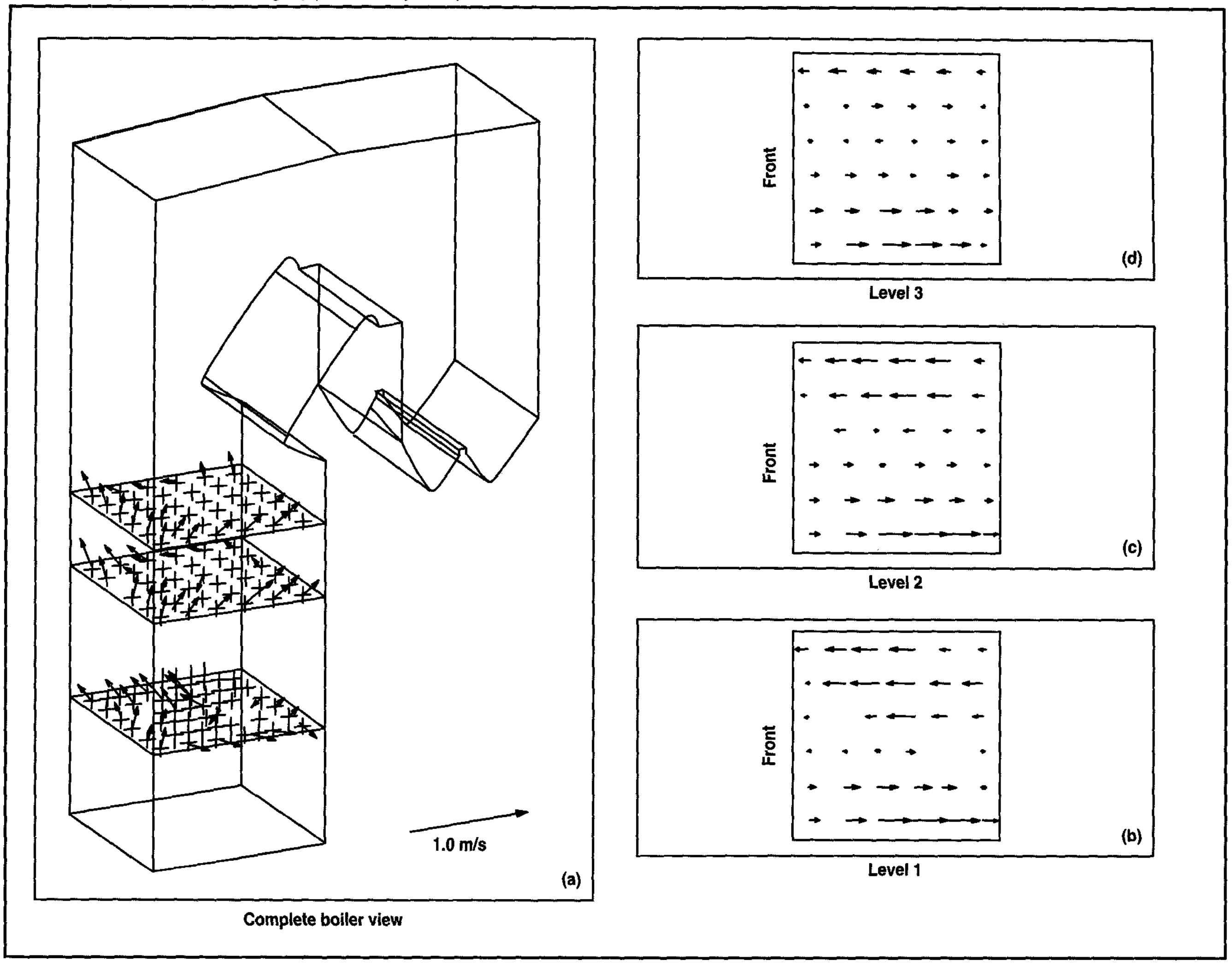

where

V_p = port flow fluid velocity, m/s

V_v = vertical flow fluid velocity, m/s

ρ_v = vertical flow fluid density, kg/m^3

ρ_p = port flow fluid density, kg/m^3

fs = subscript indicating full-scale.

The LDV used for measurements was a two-component differential beam system using a burst-correlator processor. A 1-Watt continuous-wave argon-ion laser was used as the light source. Horizontal velocity measurements (u) were made using the green (514.5-nm) line, and vertical velocities (w) were obtained with the blue (488.0-nm) line. In principle, the system is expandable to simultaneously measure three velocity components using the violet (476.0-nm) laser line. The attenuation of both incident and reflected light by the water requires the use of a relatively high power laser. The measurement volume is examined from one side of the model using a probe operating in the backscatter mode and connected to the optical bench through a fiber-optic link. Frequency shifting is used to measure negative and near-zero velocities.

The measurement volume for the LDV is located at the point of intersection of the shifted and unshifted beams emitted from the probe, and is coincident for both velocity components. It is ellipsoidal in shape, with axes of approximately 2.0 and 0.2 mm. The Doppler signal is a constant-frequency signal of Gaussian amplitude profile. The burst-correlator processor computes a correlation function between successive burst zero-crossings; if eight successive cycles correlate, the signal is deemed a valid Doppler burst and not random noise. In this way, large particles cannot cause spurious data because they cannot generate a sufficient train of bursts to satisfy the processor.

The flow was not seeded with artificial particles because the unfiltered tap water possessed suitable scattering particles of approximately 50 µm in diameter. While higher data rates could have been obtained using artificial seeding, the potential problems of blockage in small ports and flowmeters, and contaminating the model

4. Contours of nondimensionalized mean vertical velocity—Run A (Level 1)

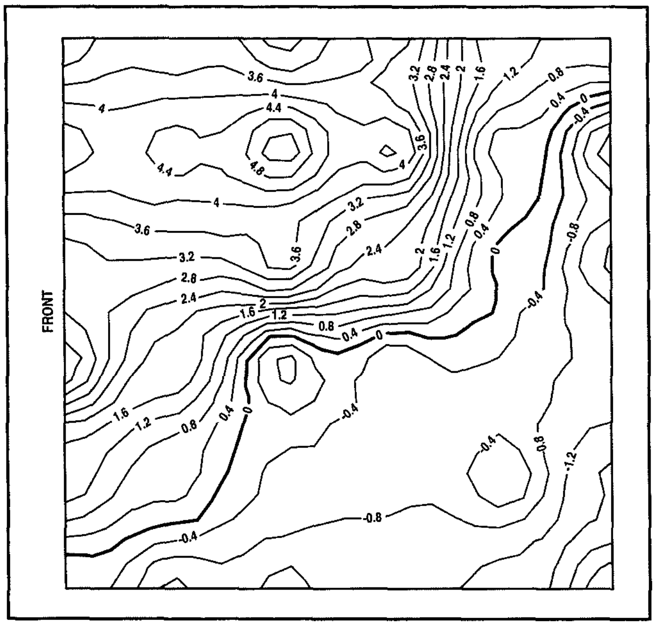

5. Contours of nondimensionalized mean vertical velocity—Run A (Level 2)

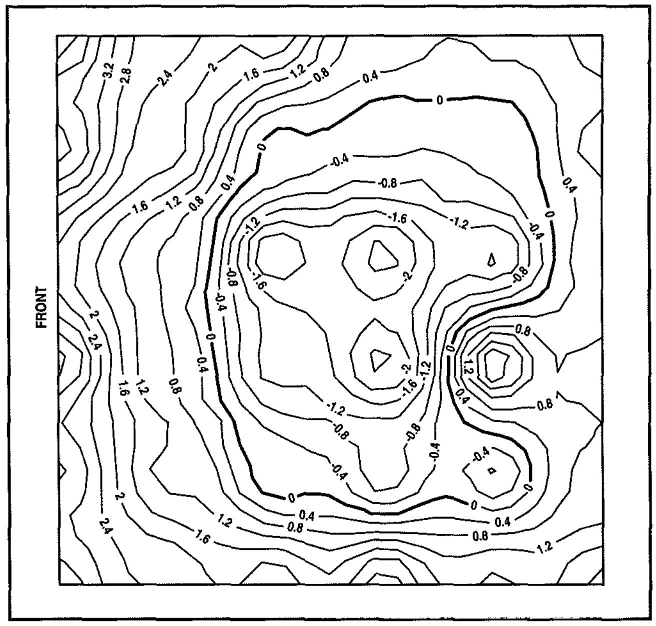

6. Contours of nondimensionalized mean vertical velocity—Run A (Level 3)

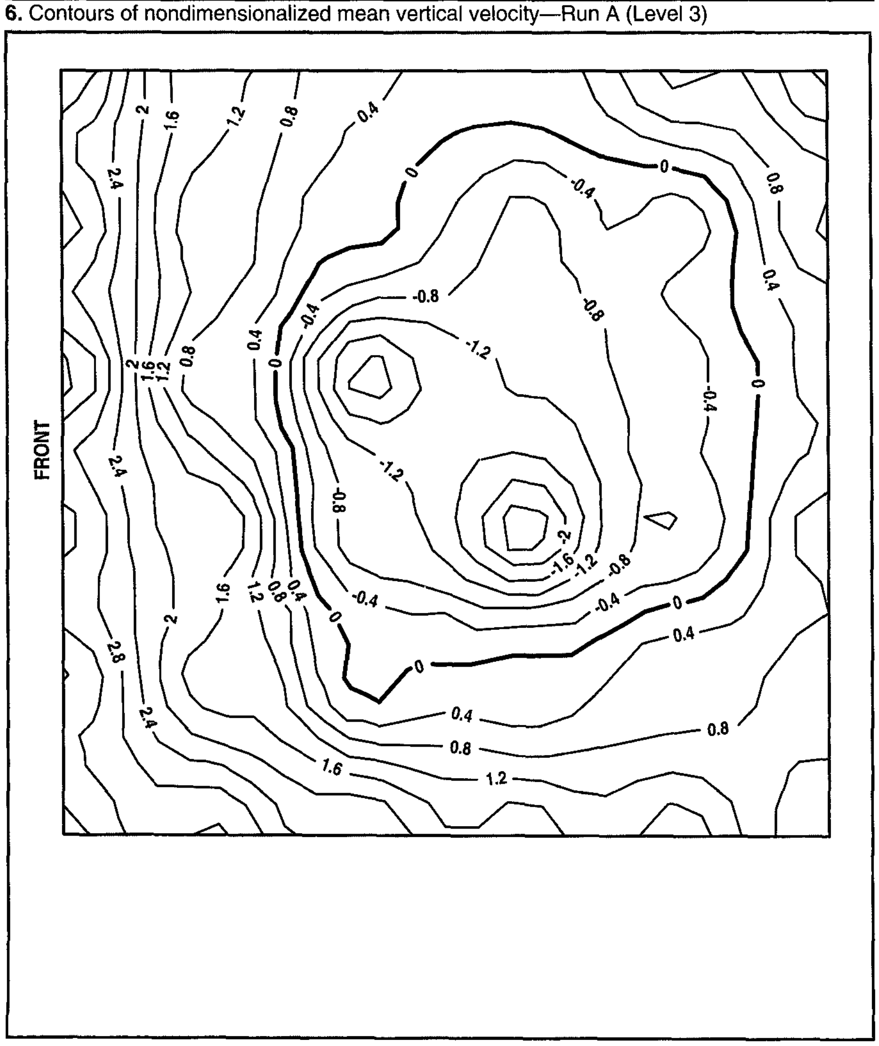

itself, outweighed any potential benefits. With natural seeding, data rates of between 200 and 2000 samples per second were attained at the model center and near the model walls, respectively.

Simultaneous measurements were made of the instantaneous velocity components in the x and z directions. Mean and root-mean-square velocities were found by averaging the data over a time long enough to smooth out the turbulent fluctuations, but short enough to retain any unsteadiness or trends in the data. When using the LDV, an averaging time cannot be specified because the data rate is a random variable; a sample size must instead be specified. At regions of the flow exhibiting low and high data rates, approximately 2500 and 20,000 data points were collected respectively to give an approximately constant averaging time. The velocity information provided by the LDV is not a continuous signal, so bias in the estimated velocities was eliminated by weighting the raw velocity values by the residence time of each particle in the measurement volume:

7. Two components of mean and RMS velocities—Run B. (a): RMS *u* and *w* velocities are shown as crosses originating from the base of each mean velocity vector, (b) through (d): *u* velocity component alone is shown for the three measurement levels.

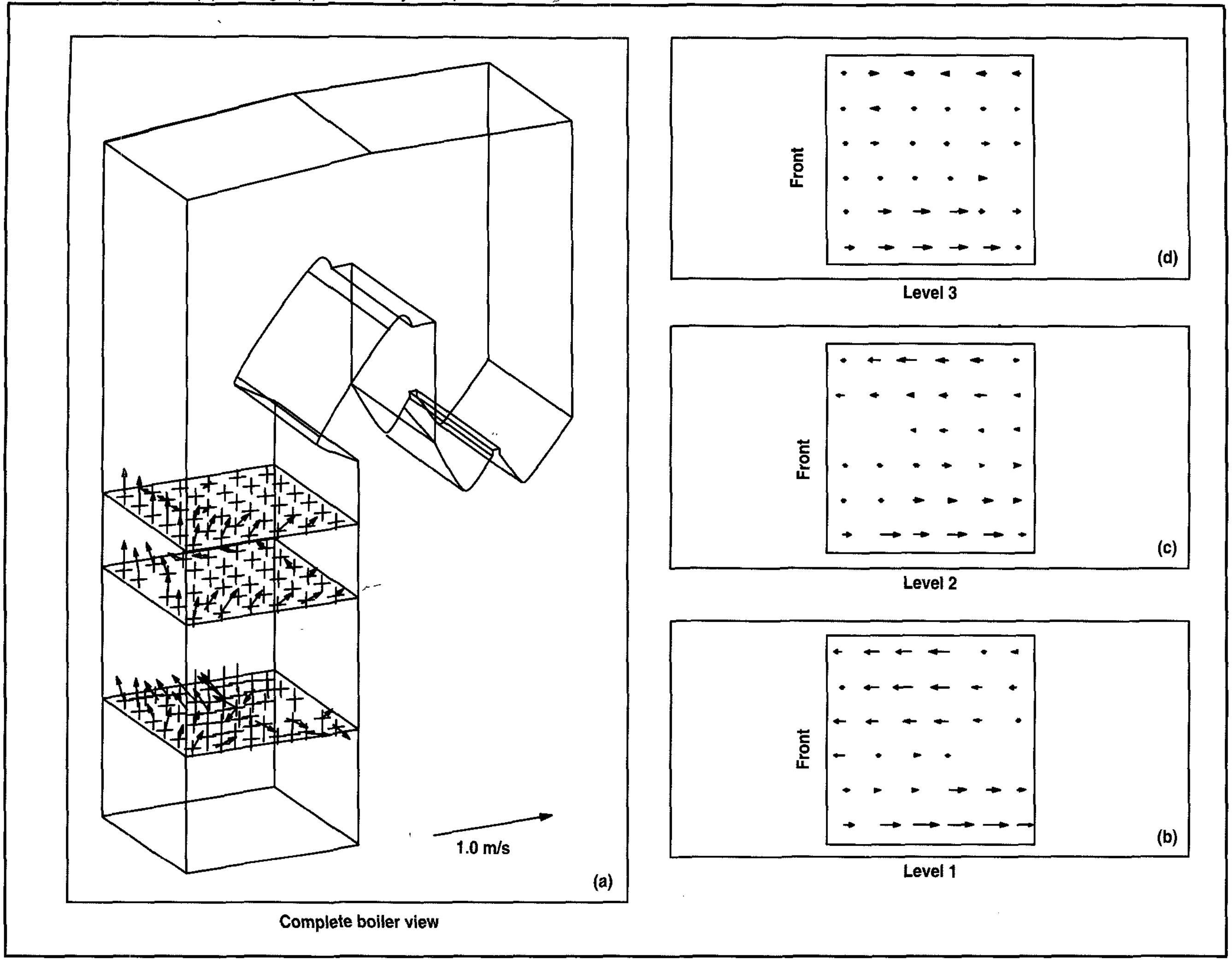

$$\bar{u} = \frac{\sum_{i=1}^{n} u_i \Delta t_i}{\sum_{i=1}^{n} \Delta t_i} \qquad (2)$$

where

$\bar{u}$ = mean horizontal or vertical velocity, m/s

u_i = i-th velocity measurement, m/s

Δt_i = duration of the i-th velocity measurement, s

Measurements were taken using a load-burner flow configuration with mass flow percentages through each set of ports approximating a typical condition in the full-scale boiler. Configurations using the tertiary ports have not yet been run. Runs were made with and without the starter burners in use, with different load-burner velocities, and with two total water flow rates. At the higher flow rate, velocities at the port exits should be approximately 0.8 m/s for the starting burners, 2.0 m/s for the primaries and load burners, and 3.4 m/s for the secondaries. One run was made with the Plexiglas plates, which model the boiler tubes, removed. Two-dimensional velocity information was obtained on three horizontal planes of 36 points each. Horizontal planes were divided into 6 x 6 grids of equal areas, the center of each being the measurement location. As shown in Fig. 2, these levels are near the liquor guns, above the load burners and below the bull nose. Qualitative flow visualization was performed to confirm the gross features of the flows.

Results

At the time of writing, approximately a dozen runs had been performed for variations of the load-burner configuration; the results from three variations are presented here. Reynolds numbers in the full-scale and model boilers are sufficiently high to ensure fully turbulent flow. The Reynolds number effects in fully turbulent flow are small, so the actual total water flow rate in the model should not be critical as long as it remains above

8. Contours of nondimensionalized mean vertical velocity—Run B (Level 1)

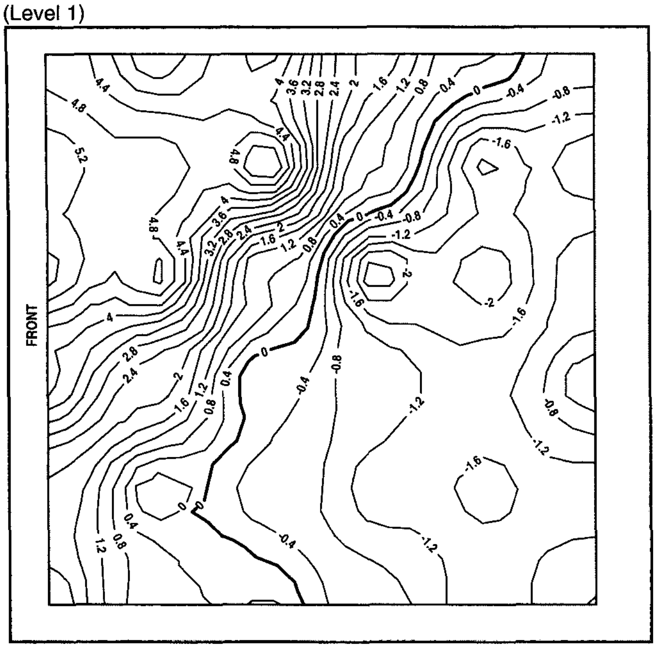

9. Contours of nondimensionalized mean vertical velocity—Run B (Level 2)

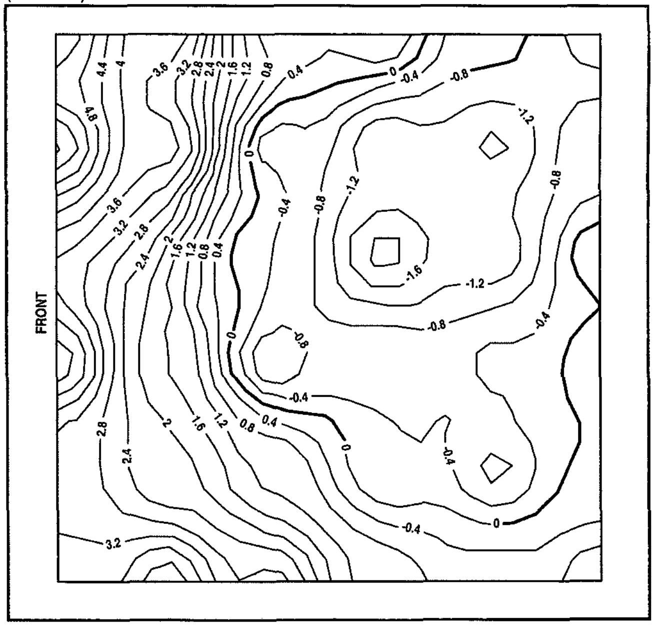

10. Contours of nondimensionalized mean vertical velocity—Run B (Level 3)

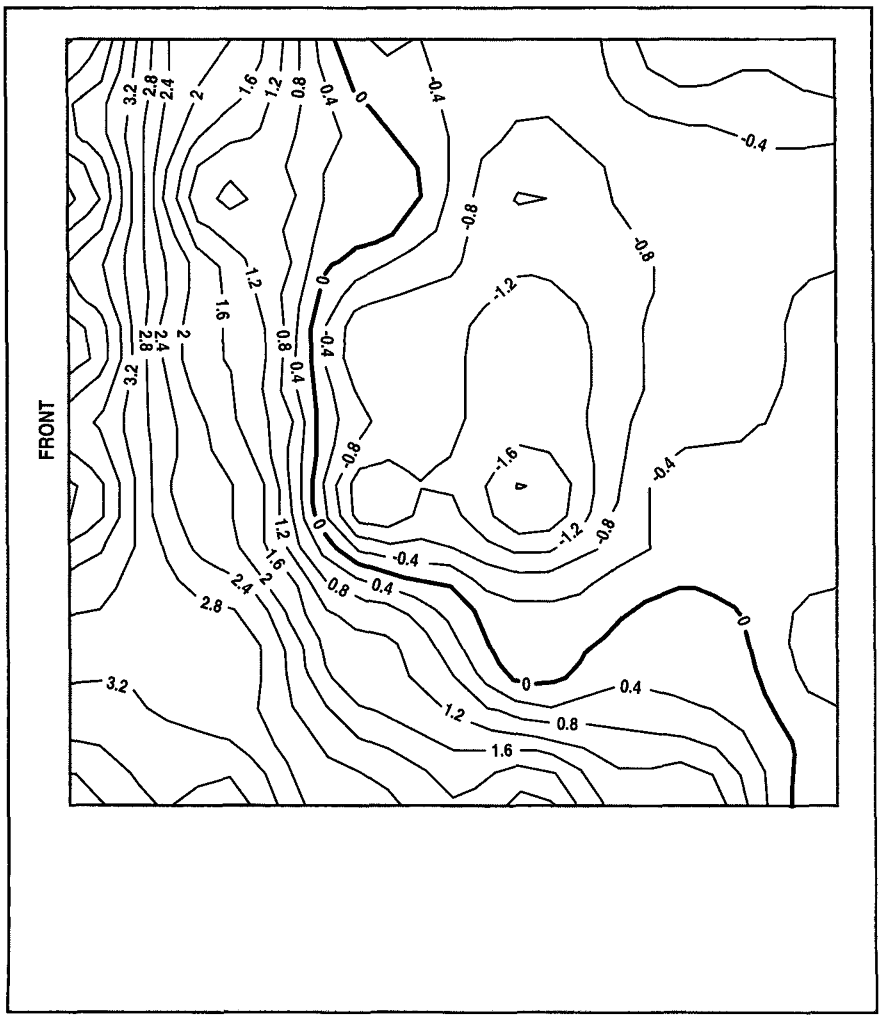

some threshold value. Run A was conducted with the starting burners in use. Run B did not use starting burners and was at the lowest flow rate possible in the facility. The effects of removing the Plexiglas plates, which model the screen and boiler tubes, are shown in Run C. A measure of the turbulence in the flow is the turbulence kinetic energy, which may be defined as:

$$K' = 0.5\left(2\overline{u'u'} + \overline{w'w'}\right) \qquad (3)$$

where

K' = turbulence kinetic energy, m^2/s^2

u' = turbulent fluctuation of velocity in x direction, m/s

w' = turbulent fluctuation of velocity in z direction, m/s.

In Eq. 3, the contributions due to velocity components in the x-y plane are assumed equal. Results for the three runs being considered are shown in **Table II**.

The average vertical velocities shown in the table indicate the bulk average vertical velocity at each level. The square root of the turbulence kinetic energy is a velocity scale of the

11. Two components of mean and RMS velocities—Run C. (a): RMS *u* and *w* velocities are shown as crosses originating from the base of each mean velocity vector, (b) through (d): *u* velocity component alone is shown for the three measurement levels.

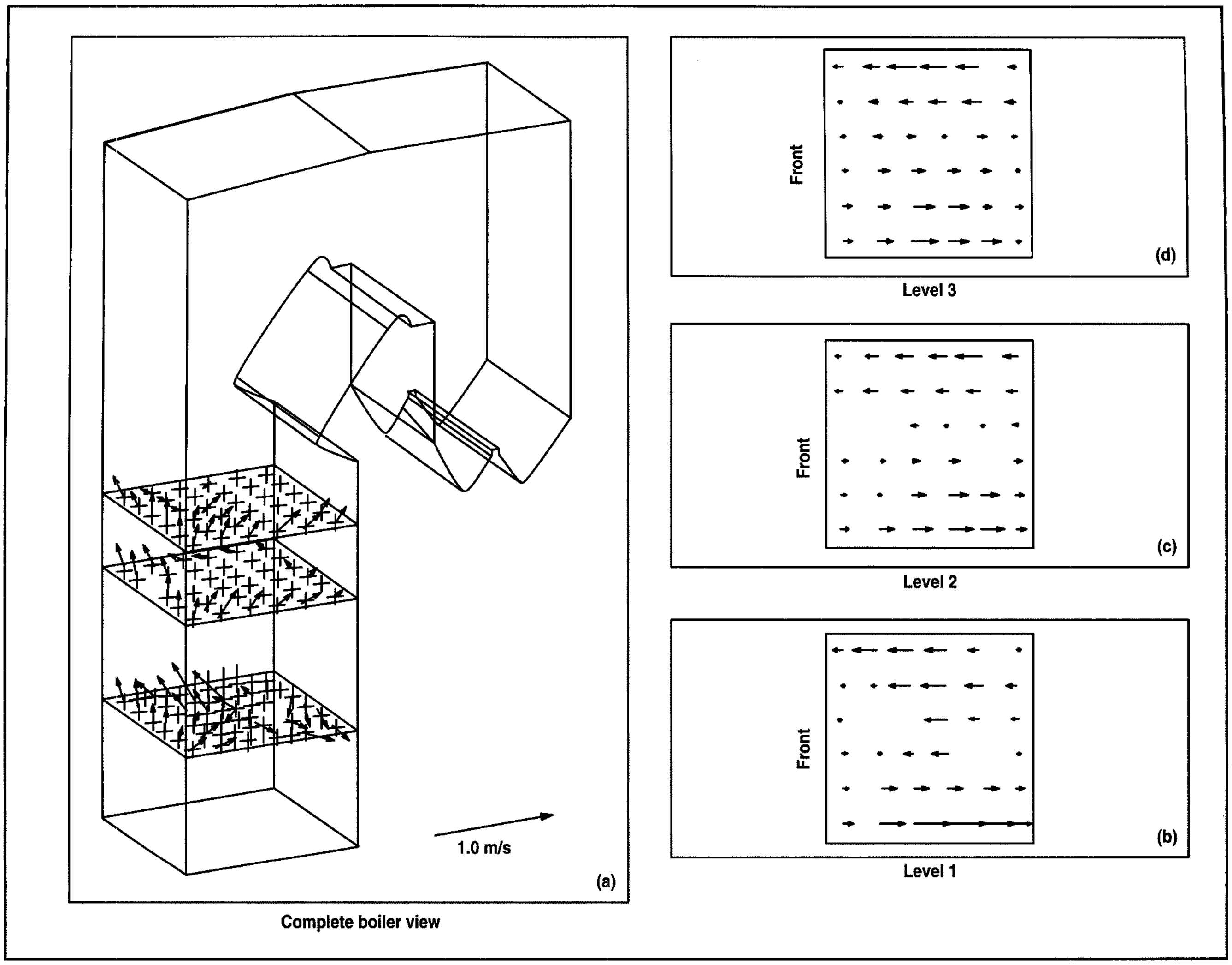

turbulence. Note that the turbulence velocity scale is always higher than the bulk average vertical velocity, ranging from about a factor of three at the lower level to a factor of 1.5–2 at the upper level. Measured flow rates at each level were found from the bulk average vertical velocity and the cross-sectional area of the model. Predicted and measured flow rates agree within about 10% for all runs.

In Fig. 3, the root-mean-square (RMS) u and w velocities are shown as crosses originating from the base of each mean velocity vector. The u velocity component alone is shown in **Figs. 3b–d** for the three measurement levels. The turbulence intensity (RMS divided by mean velocity) may be seen visually at each measurement point. Caution should be used in interpreting this figure, as the v velocity component is absent. Note that some points do not show a velocity vector because the data rate at these points was insufficient for an accurate measurement. In some cases, this may be due to the velocity being mainly in the y direction; this would appear as zero u velocity to the LDV. Contour plots of the mean vertical velocity at each point, nondimensionalized by the bulk average vertical velocity at that level, are shown in **Figs. 4–6** for levels 1 through 3, respectively.

The measured mean and fluctuating velocities for Run A are shown in vector form in **Fig. 3a.** Measured mean and fluctuating velocities, and contours of nondimensionalized mean vertical velocities, are shown in **Figs. 7–10** for Run B, and in **Figs. 11–14** for Run C, respectively.

The results shown in Figs. 3–6 are generally representative of the trials run to date. Altering the load-burner velocity, total flow rate, or the presence of boiler tubes did not affect the results significantly. (Refer to Figs. 7–14.) The removal of the boiler tubes, however, increased the swirl present in the uppermost level. At the lowest level, the majority of the vertical flow is in the front left corner of the boiler, with recirculating or downflow elsewhere. The middle and upper levels show strong vertical flow on the front and right side walls with a weak core of downflow in the central region. Turbulence intensities are higher in the

12. Contours of nondimensionalized mean vertical velocity—Run C (Level 1)

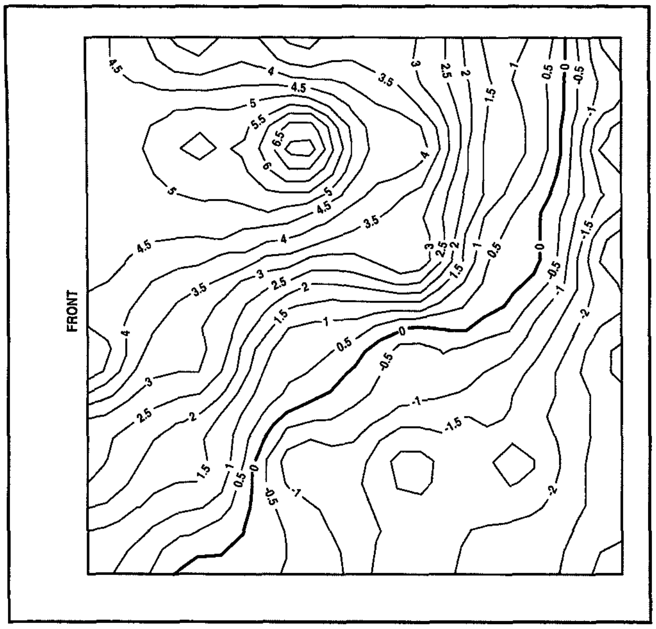

13. Contours of nondimensionalized mean vertical velocity—Run C (Level 2)

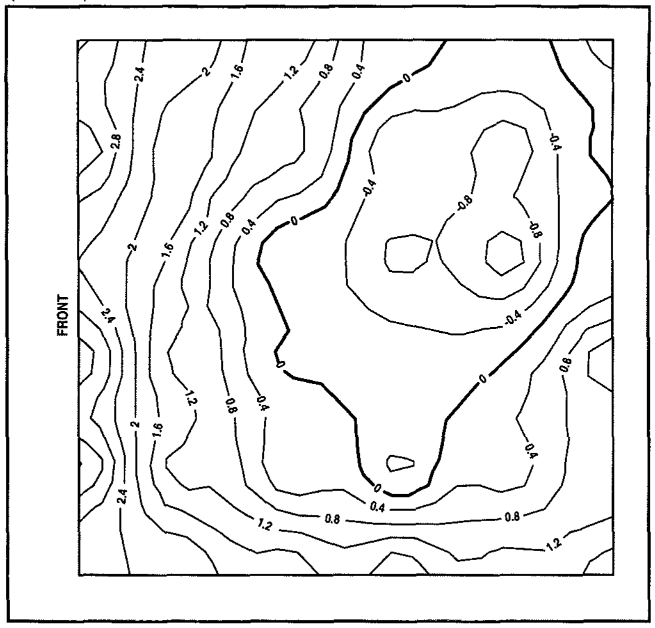

14. Contours of nondimensionalized mean vertical velocity—Run C (Level 3)

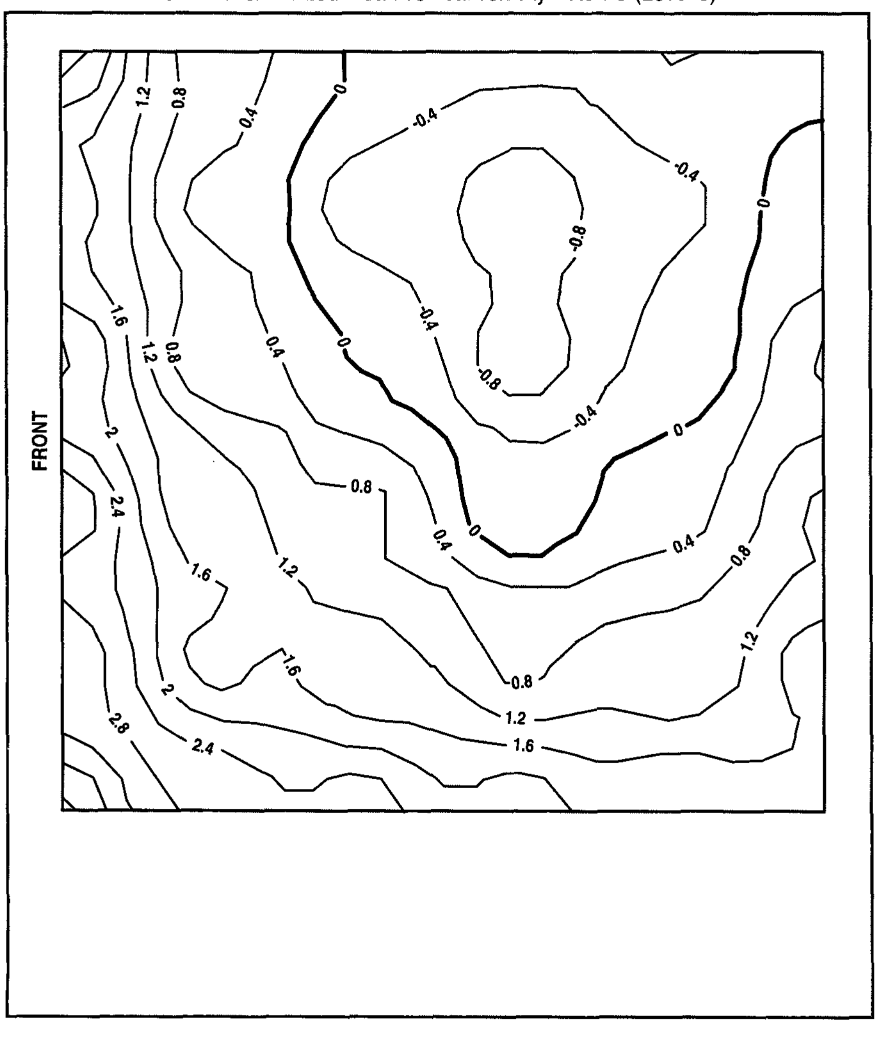

center of the boiler than near the walls, ranging from approximately 50% to 500% in each velocity component.

Traditional expectations of boiler flow involve a central channel of upwardly rising flow surrounded on all sides by recirculating flow *(10)*. Such results have not as yet been observed in the experimental facility. The lack of a smelt bed shape in the furnace may be a contributing factor to the observed flow, or it may be particular to the use of the swirl-inducing load-burner ports. Some unsteadiness has been observed while monitoring the velocity data from the LDV in real time. This usually appears in lower regions of the furnace near the walls. The unsteadiness has a large amplitude, with a period on the order of one second. A slide projector illuminating a plane of the model was used to visually confirm the regions of vertical and recirculating flow.

Future plans

Work is ongoing in the boiler model facility. Plans are being made to take measurements with different port mass flow ratios, to use the tertiary instead of load-burner ports, and to insert a smelt bed shape in the model.

Additional qualitative and quantitative flow visualization work will be performed. Similar experiments will be performed on the Kamloops boiler model, and results from both models will be compared to those of other experimenters. Computational simulations of both models are under development by researchers at UBC.

Conclusions

Measurements have been made of two components of the fluctuating velocity in an isothermal water model of a kraft recovery boiler. The results are shown to be repeatable within experimental tolerances and in the qualitative nature of the flow patterns. The use of a load-burner port tangential-flow arrangement in the upper furnace resulted in an asymmetrical flow pattern, with downflow in the central region of the boiler. A symmetrical core of vertical upflow was not observed. Minor changes in flow configuration did not significantly change the resulting flow. TJ

Literature cited

1. Walsh, A., Jones, A., Sumnicht, D., *et al.*, *TAPPI 1989 International Chemical Recovery Conference Proceedings,* TAPPI PRESS, Atlanta, p. 1.
2. Chapman, P. J. and Jones, A. K., *TAPPI 1990 Engineering Conference Proceedings,* TAPPI PRESS, Atlanta, p. 193.
3. Jones, A. K., Grace, T. M., and Monacelli, T. E., *Tappi J.* 72(5): 193(1989).
4. Holdeman, J. D., Srinivasan, R., and Berenfeld, A., *AIAA Journal* 22(10):1436(1984).
5. Pankhurst, R. C. and Holder, D. W., *Wind Tunnel Technique,* 2nd ed., Sir Isaac Pitman & Sons, London, 1968, pp. 204–211.
6. Lomas, C. G., *Fundamentals of Hot Wire Anemometry,* Cambridge University Press, Cambridge, 1986, pp. 190-195.
7. Fingerson, L. M., Adrian, R. J., Menon, R. K., Data Analysis, Laser Doppler Velocimetry and Particle Image Velocimetry, TSI Short Course Text, TSI Inc. St. Paul, MN, 1991, pp. 1-16.
8. Sacher, P.W., ed., 1987 *AGARD Conference Proceedings No. 413,* North Atlantic Treaty Organization, Nevilly sur Seine, France, p. 1.
9. Blackwell, B., Olivier, R., and Briscoe, B., *1989 CPPA Technical Section Proceedings: Pacific-Western Branches,* Canadian Pulp and Paper Association, Montreal, p. 1.
10. Adams, T. N. and Frederick, W. J., *Kraft Recovery Boiler Physical and Chemical Processes,* American Paper Institute, Inc., New York, 1988, 159.

This research was funded in part by the Weyerhaeuser Paper Co.; the Natural Science and Engineering Research Council; the Department of Energy, Mines, and Resources; and the Industry, Science, and Trade Council. The authors wish to thank Mr. K. Zhang for his assistance with the development of the experimental facility.

Received for review July 8, 1992.

Accepted Feb. 25, 1993.

Presented at the TAPPI 1992 Engineering Conference.